DOI https://doi.org/10.1016/j.jsb.2012.12.001

Genesis of amorphous calcium carbonate containing alveolar plates in the ciliate *Coleps hirtus (Ciliophora, Prostomatea).*

Marie-Louise Lemloh[1*], Frédéric Marin[2], Frédéric Herbst[3], Laurent Plasseraud[4], Michael Schweikert[1], Johannes Baier[5], Joachim Bill[5] and Franz Brümmer[1]

[1] University of Stuttgart, Biological Institute, Zoology, Pfaffenwaldring 57,70569 Stuttgart, Germany
Marie-Louise.Lemloh@bio.uni-stuttgart.de
Michael.Schweikert@bio.uni-stuttgart.de
franz.bruemmer@bio.uni-stuttgart.de

[2] UMR CNRS 6282 Biogéosciences, Université de Bourgogne, 6 Bd Gabriel, 21000 Dijon, France
frederic.marin@u-bourgogne.fr

[3] ICB - UMR 5209 – DAI, Université de Bourgogne, UFR Sciences et Techniques, 21000 Dijon, France
frederic.herbst@u-bourgogne.fr

[4] ICMUB, UMR CNRS 6302, Faculté des Sciences Mirande, Université de Bourgogne, 21000 Dijon, France
laurent.plasseraud@u-bourgogne.fr

[5] University of Stuttgart, Institute for Materials Science, Heisenbergstraße 3, 70569 Stuttgart, Germany
baier@imw.uni-stuttgart.de
bill@imw.uni-stuttgart.de

*corresponding author:
Marie-Louise.Lemloh@bio.uni-stuttgart.de

Abstract

In the protist world, the ciliate *Coleps hirtus* (phylum *Ciliophora*, class *Prostomatea*) synthesizes a peculiar biomineralized test made of alveolar plates, structures located within alveolar vesicles at the cell cortex. Alveolar plates are arranged by overlapping like an armour and they are thought to protect and/or stiffen the cell. Although their morphology is species-specific and of complex architecture, so far almost nothing is known about their genesis, their structure and their elemental and mineral composition. We investigated the genesis of new alveolar plates after cell division and examined cells and isolated alveolar plates by electron microscopy, energy-dispersive X-ray spectroscopy, FTIR and X-ray diffraction. Our investigations revealed an organic mesh-like structure that guides the formation of new alveolar plates like a template and the role of vesicles transporting inorganic material. We further demonstrated that the inorganic part of the alveolar plates is composed out of amorphous calcium carbonate. For stabilization of the amorphous phase, the alveolar vesicles, the organic fraction and the element phosphorus may play a role.

Key words: Protozoan, Ciliate, *Coleps hirtus*, alveolar plates, amorphous calcium carbonate, biomineralization

Introduction

Although far less investigated than its metazoan counterpart from a biomineralization viewpoint, the protist world is characterized by a fascinating diversity of biomineralized intracellular and extracellular structures and a variety of morphologies. That goes together with a strikingly high degree of control that these single-celled organisms exert on their mineral deposition (Lowenstam, 1986; Pautard, 1970; Simkiss and Wilbur, 1989). Most of the studies on protist biomineralization focus on coccolithophore algae, on diatoms or on Foraminifera. Beside these well-studied models, several other protist clades elaborate a complex mineralized test but their study is still in its infancy. Among these 'poor relations', one finds the planktonic protozoans of the genus *Coleps* (Ciliophora, Prostomatea) that live in marine and freshwater habitats all over the world. They swim at moderate speed, moving their barrel-shaped body turning on the longitudinal axis and they feed on algae, bacteria, ciliates and small invertebrates (Foissner et al., 1999; Noland, 1925). One specific character for the genus *Coleps* is the species-specific morphology of their biomineralized alveolar plates. These plates, also called 'crustules' by Fauré-Fremiet and coworkers (1968) are observed within alveolar vesicles (alveoli), vacuole-like structures that are located directly beneath the plasma membrane. Maupas (1885) first described in detail the so-called 'armour' built up from the alveolar plates. One *Coleps hirtus* cell is covered by six different girdles composed of several alveolar plates; the circum-oral plates, anterior secondary plates, anterior main plates, posterior main plates, posterior secondary plates and caudal plates (Fig. 1) (Foissner et al., 1999; Huttenlauch, 1985; Maupas, 1885; Noland, 1925). The number of plates per ring is variable (12-20) while the number and morphology of the so-called 'windows' (Fig. 1b), the position of the ridge and the spines of the caudal plates are species-specific (Foissner et al., 1999; Kahl, 1930).

One key-question concerns the genesis of armour plates during cell division. When *C. hirtus* cells divide, the armour is distributed equally to the daughter cells, each of them keeping one half of the test, the anterior rings or the posterior rings respectively. Then, each of them reconstitutes the missing half. The genesis of the alveolar plates and the involved cellular processes are not known so far. Moreover, the exact material and composition of the alveolar plates remain unsolved. Maupas (1885) performed detailed studies on alveolar plates including acid treatments and found out that they are rather unstable. Alveolar plates of *C. hirtus* were also studied by Fauré-Fremiet and colleagues in the forties and later on, in the sixties (Fauré-Fremiet and Hamard, 1944; Fauré-Fremiet et al., 1948; Fauré-Fremiet et al., 1968). They observed electron dense (desmosome-like) areas at some parts of the alveolar membranes in contact with alveolar plates. They proposed that these structures might act as a matrix (Fauré-Fremiet et al., 1968). They burned alveolar plates, treated them with acids and alkali and performed initial x-ray analysis (Fauré-Fremiet and Hamard, 1944; Fauré-Fremiet et al., 1948) concluding that the substance is a mineral and that amorphous calcium carbonates as well as di-calcium phosphates are present. Subsequent cytochemical staining led them to the conclusion that the plates are built from calcium phosphocarbonates linked to a polysaccharide substrate (Fauré-Fremiet et al., 1968).

One aim of our study was to identify and characterized further the mineral material with modern methods. In the present study we combined transmission and scanning electron microscopy, energy-dispersive X-ray spectroscopy, X-ray diffraction and FTIR to examine the genesis and the nature of the mineral part for alveolar plates of *C. hirtus*.

Material and Methods:

Sample collection and documentation of dividing stages

C. hirtus cells were collected from Trentsee (Plön) in Germany and cultured for several years under controlled conditions before alveolar plates were isolated and stored dry and frozen, according to a recently published procedure (Lemloh et al., 2012). Briefly, *C. hirtus* cells were homogenized in phosphate buffer containing a protease inhibitor mix and alveolar plates were afterward collected by a series of washing and sedimentation steps in cold acetone. To improve the chance of observing cells immediately after division, the culture was starved for one week: subsequent feeding led to increase cell division 12 h later. Dividing cells still in connection were collected at t=0. Cells were subsequently sampled at 30, 60, 85, 135, 195 and 255 min after T_0. All samples were processed for SEM/TEM observations.

SEM Observations

Samples were air dried on silicon weavers before sputter coating with 1 nm Pt/Pd. Scanning Electron Microscopy observations were performed with a Zeiss Gemini DSM 982 Scanning Electron Microscope (Zeiss) at 3 kV. Complementary observations were performed with a Jeol JSM 760 F field emission scanning electron microscope (Jeol Ltd., Tokyo, Japan), after carbon sputtering of the sample surfaces (8V, 100 A by 3 to 5 sec flash) to a thickness of 15 nm, controlled by a quartz balance.

TEM

For transmission electron microscopy (TEM) samples were fixed with glutaraldehyde and osmium as described by Huttenlauch and Bardele (1987) except for using phosphate buffer at a pH 9. Cells were rinsed in phosphate buffer pH 9 and dehydrated in an ethanol series. Ethanol (Carl Roth GmbH, Karlsruhe, Germany) was replaced by 1,2-Epoxypopan (Roth) before samples were embedded in Epon (Roth). Ultrathin sections were prepared using a diamond knife on an ultramicrotome (UCT Ultracut,Leica, Wetzlar, Germany). Sections were observed at a Zeiss EM 10 (Carl Zeiss AG, Oberkochen, Germany) (electron source: W) at an acceleration voltage of 60 kV and images were

taken using Kodak 4489 film. Semi-thin sections (around 200 nm) were documented at a FEI Tecnai G2 (FEI Europe, Eindhoven, Netherlands) (electron source: LaB_6) at an acceleration voltage of 200 kV using a Tietz CCD camera F-224 (Tvips, Gauting, Germany).

EDX analysis of dividing stages

EDX (energy-dispersive X-ray) spectroscopy was performed with a Jeol JSM 760 F field emission scanning electron microscope (Jeol Ltd., Tokyo, Japan). This microscope was equipped with a backscattered electron detector (COMBO). EDX elemental mappings were analysed for samples prepared after cell division (see above) that were coated with Pt/Pd as well as for single alveolar plates that were transferred to silicon weavers and 13 nm carbon coated.

XRD

Samples, which were put on silicon wafers, were measured with a PANanalytic X-pert MPD (PANalytical, Almelo, Netherlands) in Bragg-Brentano geometry, using a Co Ka radiation (40 mA and 40 kV) in a 2Θ range of 20° and 80°. In between first and second XRD (X-ray diffraction) analysis, alveolar plates were heated at 450 °C for 30 min within a DSC (differential scanning calorimetry) (DSC I, STAR System, Mettler Toledo GmbH, Giessen, Germany) for controlled heating.

FTIR

Isolated dried alveolar plates were analysed by Fourier Transform InfraRed spectroscopy (FTIR). FTIR spectra were recorded on a Bruker Vector 22 instrument equipped with a Specac Golden Gate Attenuated Total Reflectance (ATR) device (Specac Ltd., Orpington, UK) in the 4000–500 cm^{-1} wavenumber range (ten scans with a spectral resolution of 2 cm^{-1}). IR data file were baseline corrected. The assignment of absorption bands was performed by comparison with previous spectra descriptions available in the literature.

Results:

Alveolar plate organization by SEM:

As shown in Fig. 1, the species *C. hirtus* is characterized by main plates with four windows and secondary plates with two windows, respectively (Fig. 1b,c). Within the armour, plates belonging to the same plate ring overlap and the respective protrusions (named teeth) lay beneath the next plate (Fig. 1a,b). In between the teeth, a space is created for cilia emerging from the plasma membrane to facilitate movement of the cells in their aqueous environment (Fig. 1b), as it was already observed in earlier work (Chardez, 1976; Small et al., 1971).

Transmission electron microscopy of *C. hirtus* cells

C. hirtus cells were embedded for TEM using several protocols and embedding materials to obtain detailed information on the alveolar plate structure. Exclusively at pH 9, alveolar plates were preserved during fixation and embedding. A cross section of a *C. hirtus* cell is given in Fig. 2a. The alveolar plates (A) are located within alveolar vesicles in the cell cortex (membranes are indicated in Fig. 2c). The cell contains vesicles (V) with dense material (Fig. 2a,b). Semi-thin sections (Fig. 2b,c) were prepared to analyse the structure of the alveolar plates itself. However, sectioning most likely resulted in the loss of some parts of the alveolar plates. These areas appear white in alveolar plates (A) (Fig. 2b,c) and inside of some vesicles (V) within the cells (Fig. 2b). Therefore, characterization of the mineral part was performed by analysing isolated alveolar plates with x-ray diffraction.

Genesis of alveolar plates

For SEM studies, *C. hirtus* cells were air-dried. This treatment destroyed the cell membranes, exposing the alveolar plates. The genesis of the second half of the armour after cell-division was studied, and the results are shown on Fig. 3. Right after division, only one half of the daughter cells is

covered by alveolar plates (Fig. 3a). The process of alveolar plate synthesis is fast, as the newly synthesized alveolar plates cannot be distinguished from the old part within a maximum of two hours after cell division (Fig. 1a). About 30 min – 1 h after division, the new part of the armour is composed of an alveolar plate precursor that is characterized by a mesh-like structure (Fig. 3b,d). About 60 min after cell division, the old (Fig. 3c) and new (Fig. 3d) alveolar plates still show different morphology. With time, a thickening of the mesh-like structure is observed until the newly formed alveolar plates completely cover the surface of the previously 'naked half'. This process is completed after about 90 min.

Cells after division were also studied by EDX for elemental mapping. The obtained elemental maps were superimposed with images obtained with backscattered electron (BSE) mode. In this mode, zones composed of heavier elements are brighter, while those composed of light elements are darker. The results are illustrated on Fig. 4a,b and c for BSE images, and on Fig. 4d-l, for EDX mapping. Fig. 4a shows that the part of the cell that is covered with alveolar plates (left side) is built up from a more dense material (brighter), the same is true for the vesicles on the uncovered (right) part of the cell. Furthermore, these vesicles are only observable with this type of detector; surface information obtained by a secondary electron detector did not reveal these particles. This strongly suggests that these particles/vesicles are not at the surface, but inside the cell. Elemental mapping for Ca, O and P of the same cell, given in Fig. 4d,g,j, shows that the distribution of Ca and O (but not P) coincides with the localization of the alveolar plates on the left part of the cell, while that of Ca, O and P completely superimpose with the internal vesicles, on the right side of the preparation. Mg was also detected in association to the vesicles while C could not be examined for whole cells since the background was too high.

Fig. 4b displays a cell 30 min after cell division: the half of the cell covered with old alveolar plates is on the left side, as indicated by its brighter aspect in BSE mode. This difference is also observable on

the EDX map for calcium (Fig. 4e), which underlines the presence of calcium in the left half while the calcium concentration in the right half is much lower although the forming alveolar plates are apparent. Between 30 min and 2 h after cell division, one can notice an important chemical modification: on the BSE mode image of the '2 hours after cell division' sample (Fig. 4c), the right half becomes almost as bright as the left one. Furthermore, the EDX map of calcium shows a drastic increase of this element in the right newly-formed part (Fig 4f). This obviously corresponds to a rapid mineralization of the newly-formed half.

To study the composition of the alveolar plates without having the whole cell in background, isolated alveolar plates were also examined via EDX (Fig. 4h,I,k,l). The elements Ca, C and O correlate with the structure of the alveolar plates: in particular, the ridge and the windows can be recognized. Although the shape of the alveolar plate is still recognizable, the phosphorus mapping gives a more blurred and homogeneous pattern (Fig. 4k). Isolated alveolar plates were analysed also regarding the occurrence of other elements like Na, S, K, Cl or Si but these elements were not detectable via EDX.

Characterization of the mineral and organic phase

Isolated, dried alveolar plates were analysed via powder X-ray diffraction. Since none of our numerous measurements revealed diffraction patterns corresponding to a crystalline phase, we concluded that the alveolar plates are composed of an amorphous material (Fig. 5a). To test the transformation of an amorphous material into a crystalline one by heat treatment, isolated alveolar plates were heated at 450 °C for 30 min. After this treatment, the sample colour changed from white to brownish, indicating that organic parts were burnt. Heat-treated samples were again analysed by powder XRD (Fig. 5b). The XRD data revealed the appearance of crystalline calcite characterized by the strongest (104)-, (110)-, (113)-, (202)-, (018)- and (116)-reflections (ICDD card no. 05-0586). Thus it can be stated that amorphous calcium carbonate is also present within untreated sample, which is

also supported by EDX measurements of alveolar plates. The small reflection at about 47° 2Θ is due to substrate, which is present within both samples.

At last, isolated alveolar plates were characterized by FTIR, and the obtained spectrum is shown on Fig. 6. The broad band at 3214 cm^{-1} can be attributed to NH/OH functions. The characteristic amide I band at 1651 cm^{-1} is characteristic of proteins. The amide II band (also characteristic of proteins) around 1470 cm^{-1} makes a shoulder, masked by an undetermined band of higher intensity at 1403 cm^{-1}. The fact that another band at 861 cm^{-1} is also observed suggests that both absorptions (861 and 1403 cm^{-1}) characterize an amorphous calcium carbonate phase (Raz et al., 2002). The 1007 cm^{-1} broad band may be indicative of saccharidic moieties (C-C-O and C-O-C stretching (Marxen et al., 1998)). To detect the putative presence of chitin, the obtained spectrum was compared to that of chitin. Both spectra are quite different, and there is no indication that the alveolar plates contain chitin.

Discussion

Although the alveolar plate fine structure of the genus *Coleps* was described few times including the detailed observations made by Maupas (1885), Noland (1925), Fauré-Fremiet et al. (1968), Huttenlauch (1985) and finally Foissner et al. (1999), the exact composition as well as the genesis of the alveolar plates is not known so far. In the present study we focused on the mineral part of the alveolar plates. Previous observations revealed that the alveolar plates are not very resistant and sensitive to acid treatments (Fauré-Fremiet and Hamard, 1944; Maupas, 1885). This, taken together with results published by Claparède and Lachmann (1858), noticed a resistance-to-burning of the alveolar plates, strongly suggested that the plates are mineralized.

While trying different conditions for TEM preparation, we affirm that alveolar plates are sensitive to low pH values. At pH 9, we conserved the alveolar plates within the epoxy resin but during subsequent sectioning parts of the alveolar plates got lost. The fact that the alveolar plates are not very stable under certain laboratory conditions supported our assumption that an amorphous material must be present. This was confirmed by the absence of any diffraction patterns for untreated alveolar plates analysed by XRD. A heat treatment was applied to induce a phase transformation from amorphous calcium carbonate to calcite (Günther et al., 2005). This was successful and diffraction patterns characteristic for calcite were detected via XRD. Our experiments clearly demonstrate that an amorphous calcium carbonate is present in the alveolar plates of *C. hirtus*.

The finding that parts of the alveolar plates are composed of amorphous calcium carbonate (ACC) goes along with the EDX results. The elements calcium, oxygen, carbon and phosphorus co-localize in the alveolar plates. Since phosphorus did not appear within the crystal structure after heat treatment, it is most probably correlated with the organic part of the alveolar plates. In general, magnesium and phosphorus are known to stabilize ACC (Politi et al., 2010; Weiner et al., 2003) and both elements were detected in association with vesicles in *C. hirtus*. Also the organic part of the alveolar plates and the location within the alveolar vesicles might be involved in stabilizing the ACC. ACC was described for a range of different phyla and it seems to play an important role in biomineralization processes and also in the resulting biomineral (Gong et al., 2012; Seto et al., 2012; Weiner and Addadi, 2011). Nevertheless so far, an occurrence of ACC within a ciliate protective structure has not been described and this further emphasizes the widespread occurrence of ACC in very different biomineral types. Different factors can promote the stabilization of biogenic ACC: enrichment of the mineralization medium in phosphorus and magnesium, confinement, presence of small organic metabolites (citrate, pyrophosphate) or polyanionic macromolecules (glycol/phosphor-proteins, polysaccharides). However, the mechanism of ACC stabilization is still not understood

(Akiva-Tal et al., 2001; Gong et al., 2012; Politi et al., 2010; Raz et al., 2003; Stephens et al., 2010; Weiner and Addadi, 2011; Weiner et al., 2003; Williams, 1991) and therefore the mechanisms applied by a single celled organism are worthwhile to study.

One feature of *C. hirtus* is the mesh-like precursor structure (matrix) that guides the formation of new alveolar plates. The precursor structure was observed especially within the first 30-60 min of alveolar plate formation while the amount of calcium within the alveolar plates is increased with time during the 2 h of formation. The partly organic nature of the alveolar plates was also shown by the brownish colour of the isolated alveolar plates after heat treatment.

Our SEM observations and EDX mapping showed that after cell division, the half that has to be reconstituted is processed as follows: first, formation of an organic un-mineralized framework, then rapid mineralization of that framework (after 2 hours). The mechanism by which the framework is mineralized may be described hypothetically according to two modes: binding of amorphous nanoparticles, such as nanospheres to the template, or progressive 'impregnation' of the template by calcium salts. The concentration of the inorganic precursors is made via vesicles that probably migrate to the sites of mineralization.

The exact nature of the organic template is so far unknown. It was examined only by Fauré-Fremiet (1968) who, after a cytochemical staining with ruthenium red, proposed the existence of a polysaccharide template. Our FTIR investigations suggest that a polysaccharide and protein fraction may be present in the plates. There is no evidence that the saccharidic moiety is chitin. Further investigations of the organic compound as a matrix structure for biomineralization seems to be promising, although technically challenging, due to the small amount of material that one can collect.

TEM and SEM observations further displayed vesicles within the *C. hirtus* cells that might be involved in alveolar plate generation, e.g. by transporting inorganic material for plate formation. So far, we were not able to isolate the vesicles for separate investigations but calcium granules containing crystalline or amorphous material are known for other organisms (Simkiss, 1976).

What could be the advantage of using ACC for the alveolar plates? Noland (1925), and later Foissner and coworkers (1999) proposed that the armour built up from the alveolar plates functions for protection of *C. hirtus*. In this case, the incorporation of ACC could stiffen the alveolar plates. Although it is a stable armour, one have to mention that the alveolar plates are arranged in a way, that they are flexible and can adapt to the actual cell shape, for example more spherical after feeding. ACC is from an energetic viewpoint easier to synthesize than its crystalline counterparts, can be more rapidly available and subject to easy remodelling. Stabilizing ACC with biopolymers or metabolites may be more economical than producing a fully crystalline test. This hypothesis however needs to be demonstrated accurately.

Conclusion

Besides answering biological relevant questions, research on biological structures inspires material science, e.g. in terms of bio-inspired mineralization processes. In the present work we examined the biomineral within generating alveolar plates from the poorly known single celled freshwater organism, *C. hirtus*. Hereby a mesh-like precursor non-mineralized structure (matrix) for *C. hirtus,* which is most probably involved in the mineralization process, was described. Furthermore, we proved the existence of an amorphous calcium carbonate phase within the alveolar plates. This is most likely stabilized due to its microenvironment (alveolar vesicle), by an organic fraction within the plates and eventually by the element phosphorus. After cell division, we showed that the synthesis of

new alveolar plates follows a two-steps procedure: synthesis of the organic template and rapid mineralization of this template. The *C. hirtus* model emphasizes once more the importance of amorphous calcium carbonate phases – whatever they are, transient or stable – in the process of biologically-controlled mineralization (Weiner and Addadi, 2011).

Acknowledgements

Parts of this work were supported by German Research Foundation (Deutsche Forschungsgemeinschaft) Grant PAK 410 and the EU COST Action TD0903 ('Biomineralix', www.biomineralix.eu) in the frame of a Short-Term Scientific Mission of ML Lemloh (STSM TD0903-8043) in Biogeosciences, Dijon. The authors want to thank S. Hoos and S. Schmiech for their help with the *C. hirtus* culture, R.O. Schill for his support, the Stuttgart Center for Electron Microscopy (StEM) for the possibility to use the SEM and F. Predel for assistance. G. Maier (Max Planck Institute for Intelligent Systems) is thanked for XRD measurements.

References:

Akiva-Tal, A., Kababya, S., Balazs, Y.S., Glazer, L., Berman, A.,et al., 2001. *In situ* molecular NMR picture of bioavailable calcium stabilized as amorphous $CaCO_3$ biomineral in crayfish gastroliths. Proc. Natl. Acad. Sci. USA 108, 14763-14768.

Chardez, D., 1976. Étude sur *Coleps hirtus* Nitzsch (Protozoa: Ciliata). Bull. Rech. Agron. Gembloux 11, 3-10.

Claparède, E., Lachmann, J., 1858. Études sur les Infusoires et les Rhizopodes. Mém. Instit. nat. genevois 5, 1-260.

Fauré-Fremiet, E., Hamard, M., 1944. Composition chimique du tégument chez *Coleps hirtus* Nitsch. Bull. biol. Fr. Bel. 78, 136-142.

Fauré-Fremiet, E., Stolkowski, J., Ducornet, J., 1948. Étude expérimentale de la calcification tégumentaire chez un infusoire cilié *Coleps hirtus*. Biochim. Biophys. Acta 2, 668-673.

Fauré-Fremiet, E., André, J., Granier, M.-C., 1968. Calcification tégumentaire chez les ciliés du genre *Coleps* Nitzsch. J. Microsc. Paris 7, 693-704.

Foissner, W., Berger, H., Schaumburg, J., 1999. Identification and ecology of limnetic plankton ciliates.Informationberichte des Bayer. Landesamtes für Wasserwirtschaft, Heft 3/99.

Gong, Y.U.T., Killian, C.E., Olson, I.C., Appathurai, N.P., Amasino, A.L., et al., 2012. Phase transitions in biogenic amorphous calcium carbonate. Proc. Natl. Acad. Sci. USA 109, 6088-6093.

Günther, C., Becker, A., Wolf, G., Epple, M., 2005. *In vitro* synthesis and structural characterization of amorphous calcium carbonate. Z. Anorg. Allg. Chem. 631, 2830-2835.

Huttenlauch, I., 1985. SEM study of the skeletal plates of *Coleps nolandi* KAHL, 1930. Protistologica 21, 499-503.

Huttenlauch, I., Bardele, C.F., 1987. Light and electron microscopical observations on the stomatogenesis of the ciliate *Coleps amphacanthus* Ehrenberg, 1833. J. Protozool. 34, 183-192.

Kahl, A., 1930. Urtiere oder Protozoa I: Wimpertiere oder Ciliata (Infusoria) 1. Allgemeiner Teil und Prostomata. Tierwelt Dtl. 18, 1-180.

Lemloh, M.-L., Hoos, S., Görtz, H.-D., Brümmer, F., 2012. Isolation of alveolar plates from *Coleps hirtus*. Eur. J. Protistol. DOI:10.1016/j.ejop.2012.07.002

Lowenstam, H.A., 1986. Mineralization processes in monerans and protoctists, in: Leadbetter, B. S. C. and Riding, R. (Eds.), Biomineralization in Lower Plants and Animals, Clarendon Press, Oxford, pp. 1-17.

Marxen, J.C., Hammer, M., Gehrke, T., Becker, W., 1998. Carbohydrates of the organic shell matrix and the shell-forming tissue of the snail *Biomphalaria glabrata* (Say). Biol. Bull. 194, 231-240.

Maupas, E., 1885. Sur *Coleps hirtus* (Ehrenberg). Arch. de Zool. Exp. et Gén. 3, 337-367.

Noland, L.E., 1925. A review of the genus Coleps with descriptions of two new species. Trans. Amer. Micros. Soc. 44, 3-13.

Pautard, F.G.E., 1970. Calcification in unicellular organisms, in: Schraer, H. (Ed.), Biological Calcification: Cellular and Molecular Aspects, North-Holland Publishing Company, Amsterdam, pp. 105-201.

Politi, Y., Batchelor, D.R., Zaslansky, P., Chmelka, B.F., Weaver, J.C., et al., 2010. Role of magnesium ion in the stabilization of biogenic amorphous calcium carbonate: a structure-function investigation. Chem. Mater. 22, 161-166.

Raz, S., Testenière, O., Hecker, A., Weiner, S., Luquet, G., 2002. Stable amorphous calcium carbonate is the main component of the calcium storage structures of the crustacean *Orchestia cavimana*. Biol. Bull. 203, 269-274.

Raz, S., Hamilton, P.C., Wilt, F.H., Weiner, S., Addadi, L., 2003. The transient phase of amorphous calcium carbonate in sea urchin larval spicules: The involvement of proteins and magnesium ions in its formation and stabilization. Adv. Funct. Mater. 13, 480-486.

Seto, J., Ma, Y., Davis, S.A., Meldrum, F., Gourrier, A., et al., 2012. Structure-property relationships of a biological mesocrystal in the adult sea urchin spine. Proc. Natl. Acad. Sci. USA 109, 3699-3704.

Simkiss, K., 1976. Intracellular and extracellular routes in biomineralization. Symp. Soc. Exp. Biol 30, 423-444.

Simkiss, K., Wilbur, K.M., 1989. Biomineralization: cell biology and mineral deposition, Academic Press Inc., San Diego.

Small, E.B., Marszalek, D.S., Antipa, G.A., 1971. A survey of ciliate surface patterns and organelles as revealed with scanning electron microscopy. Trans. Amer. Micros. Soc. 90, 283-294.

Stephens, C.J., Ladden, S.F., Meldrum, F.C., Christenson, H.K., 2010. Amorphous calcium carbonate is stabilized in confinement. Adv. Funct. Mater. 20, 2108-2115.

Weiner, S., Addadi, L., 2011. Crystallization pathways in biomineralization. Annu. Rev. Mater. Res. 41, 6.1–6.20.

Weiner, S., Levi-Kalisman, Y., Raz, S., Addadi, L., 2003. Biologically formed amorphous calcium carbonate. Connect. Tissue Res. 44, 214-218.

Williams, N.E., 1991. A comparison of alveolar plate proteins in two species of *Euplotes*. Eur. J. Protistol. 27, 21-25.

Figure captions:

Fig. 1: SEM (scanning electron microscopy) images of armour and individual alveolar plates from *C. hirtus*, **a:** nomenclature of plate rings of the armour, COP: circum-oral plates, ASP: anterior secondary plates, AMP: anterior main plates, PMP: posterior main plates, PSP: posterior secondary plates, CP: caudal plates, scale 10 µm; **b:** main plate (external view) with 4 windows (W), teeth (T) and ridge (R), C indicates the position of a cilium in living specimen, scale: 4 µm; **c:** secondary plate (internal view) with two windows (W), scale 2 µm.

Fig. 2: TEM images of *C. hirtus* cross-section, **a:** overview cross-section indicating positions of alveolar plates (A) within alveolar vesicles and vesicles within the cell (V), scale: 4 µm, **b, c:** semi-thin sections, **b:** detail of vesicle (V) and alveolar plate (A) positions within alveolar vesicle, scale: 1 µm, **c:** detail of alveolar plate, arrow indicating membranes (alveolar vesicle and outer membrane), scale: 200 nm.

Fig. 3: SEM images of air dried samples of *C. hirtus* after cell division, **a:** freshly divided cell, only one half is covered by alveolar plates, scale: 10, **b-d:** 30 min - 1 h after cell division, **b:** mesh-like structure of new generating alveolar plates, scale 5 µm, **c:** mature alveolar plates, scale: 5 µm, **d:** new generating alveolar plates of the same cell, scale: 2 µm.

Fig. 4: SEM images (backscattered electron mode) (**a-c**), EDX elemental mapping of recently divided 'daughter cells' of *C. hirtus* (**d-f, g, j**) and of isolated alveolar plates (**h,i,k,l**). Elements are indicated in brackets; **a:** just divided cell, **b:** 30 min after cell division, **c:** 2 h after cell division, scales: 10 µm; **d-f:**

elemental mapping (EDX) of calcium for the same samples, EDX elemental mapping for oxygen (**g**) and phosphorus (**j**) (t=0 min); **h, i, k, l:** elemental mapping of isolated alveolar plates, scale: 1 µm.

Fig. 5: XRD diagrams for untreated (**a**) and heated (**b**) (450 °C) samples of isolated *C. hirtus* alveolar plates. Samples were measured on silicon wafers. The reflection at 47 ° (#) is due to the substrate. The reflections labelled in (**b**) indicate calcite.

Fig. 6: FTIR spectrum of dried, isolated alveolar plates of *C. hirtus.* The main absorption peaks are indicated (in cm^{-1}).

Figure 1

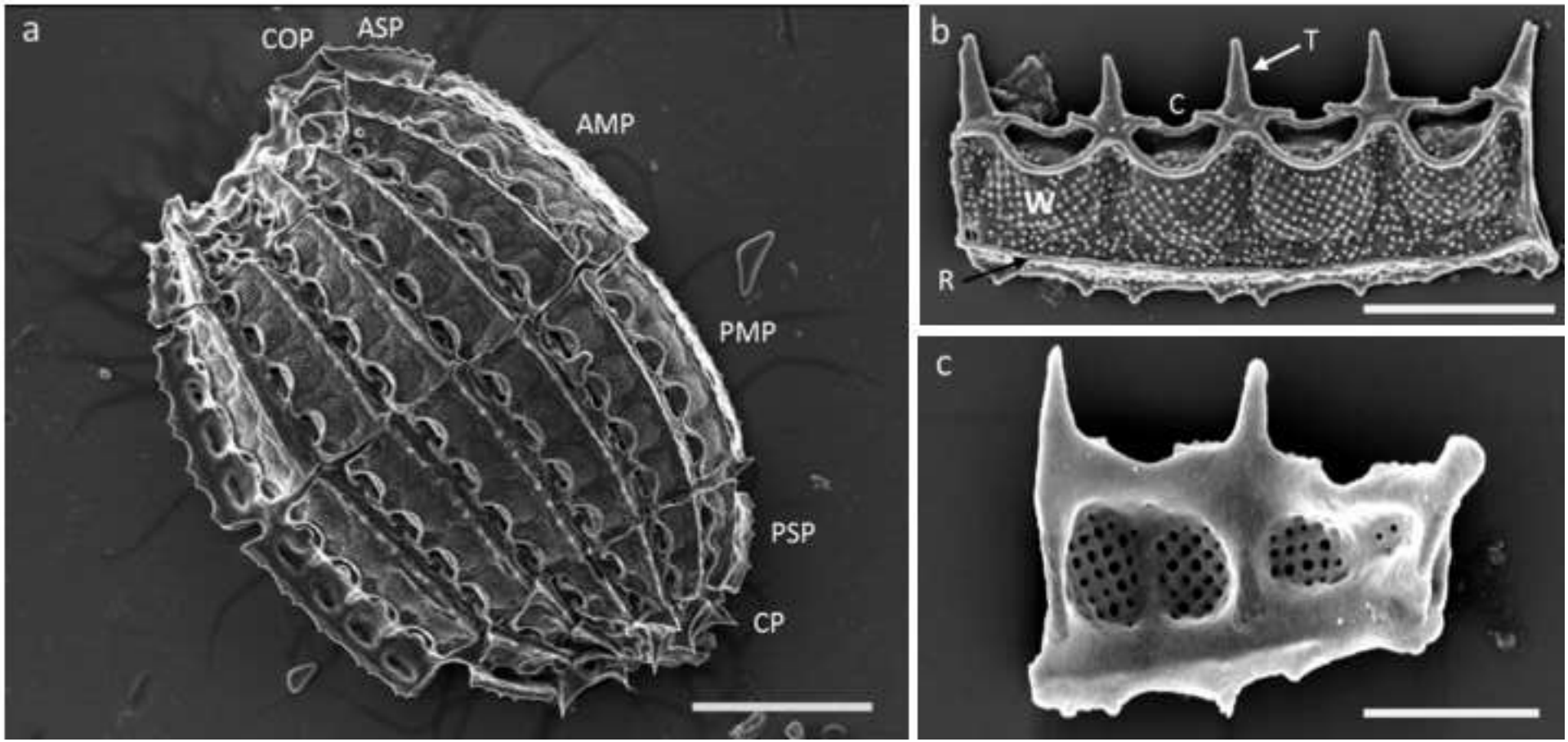

Figure 2

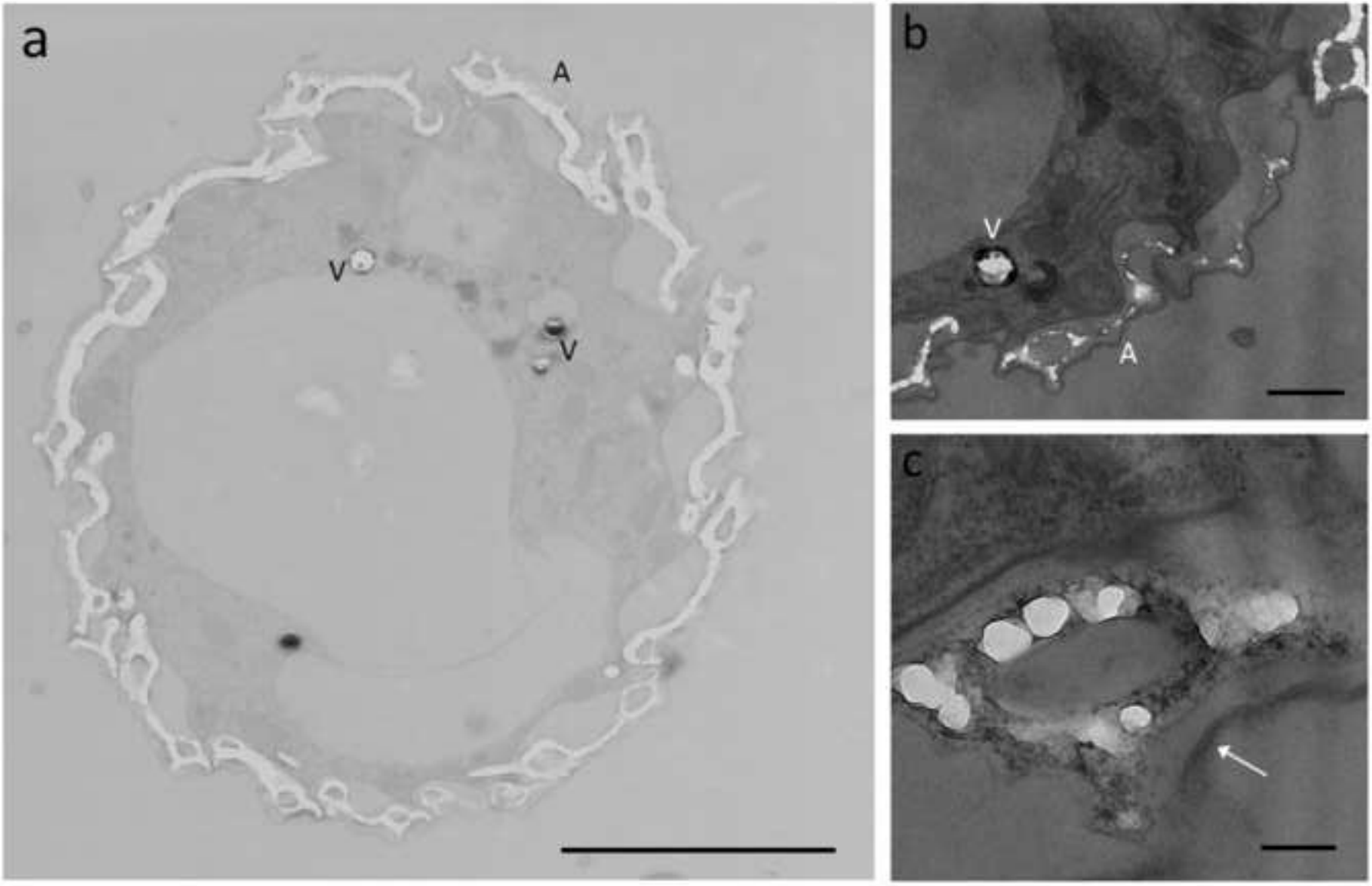

Figure 3

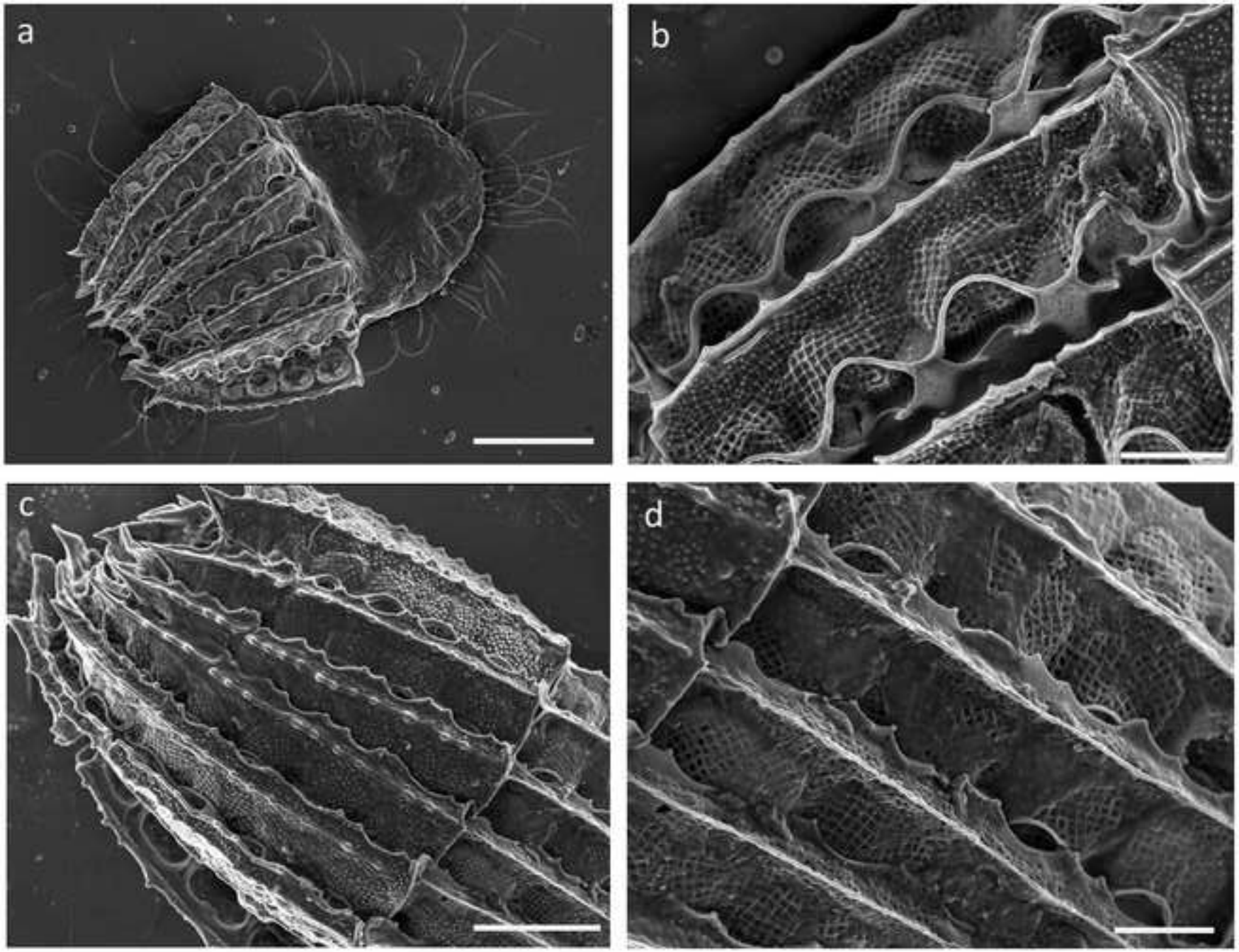

Figure 4

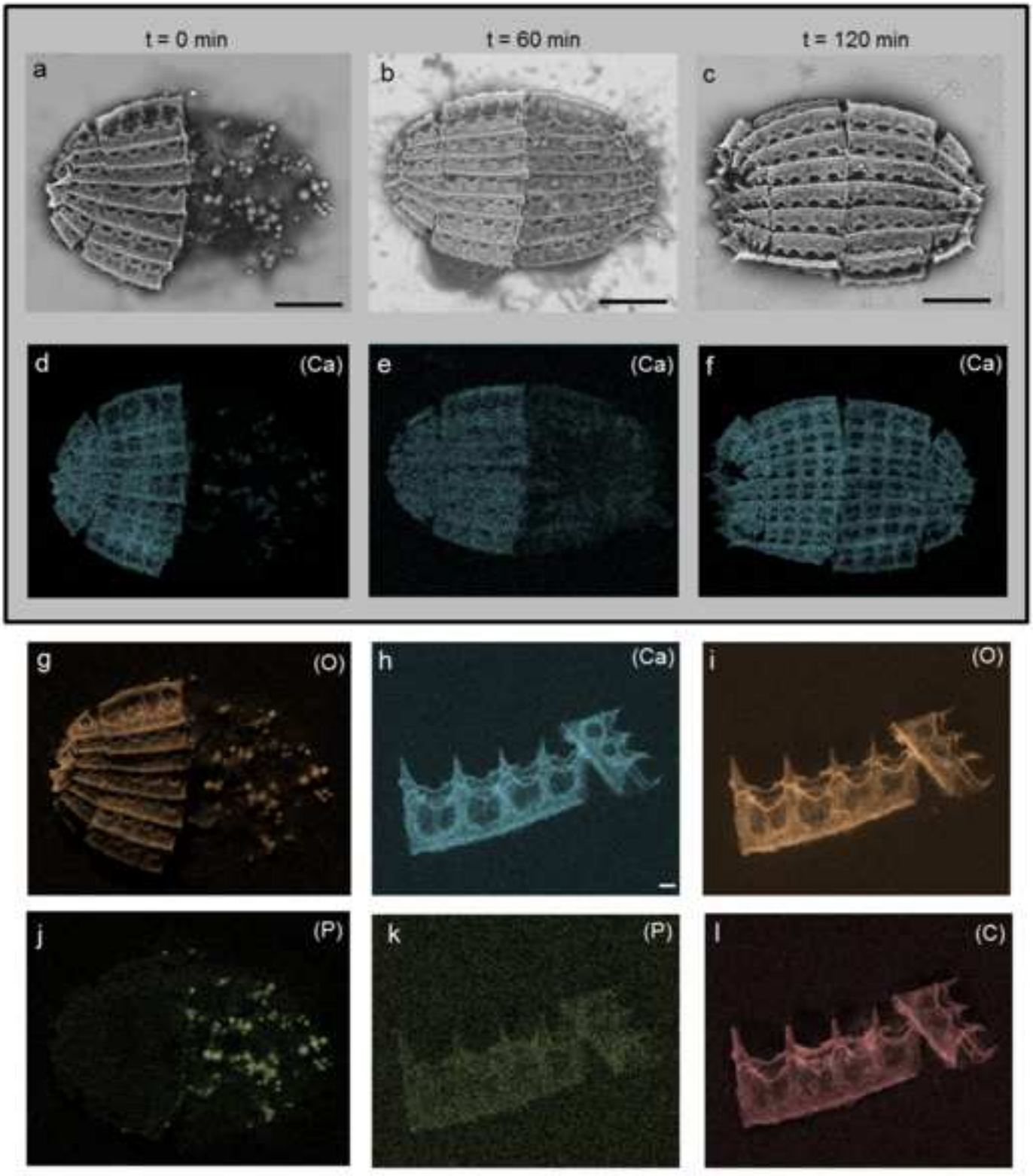

Figure 5

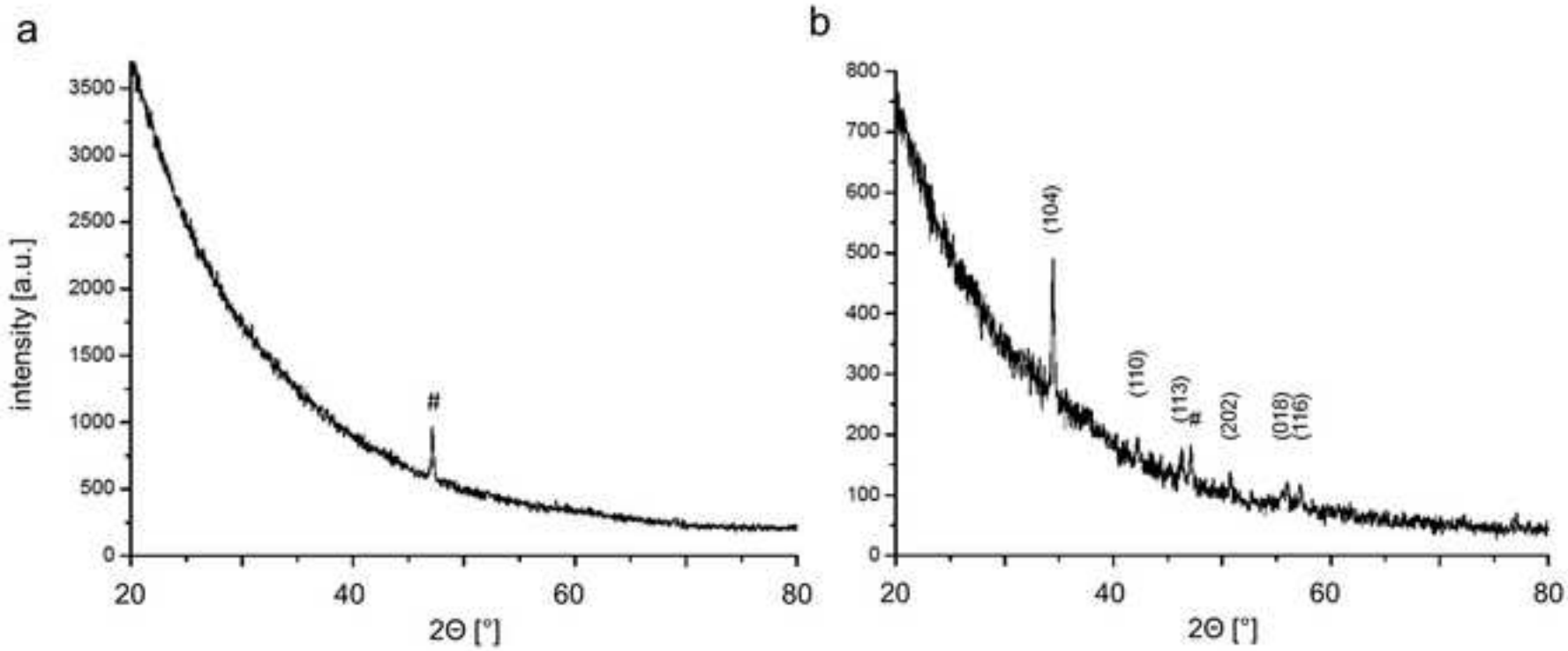
a
intensity [a.u.]
3500
3000
2500
2000
1500
1000
500
0
#
20
40
60
80
2Θ [°]
b
800
700
600
500
400
300
200
100
0
(104)
(110)
(113)
#
(202)
(018)
(116)
20
40
60
80
2Θ [°]

Figure 6

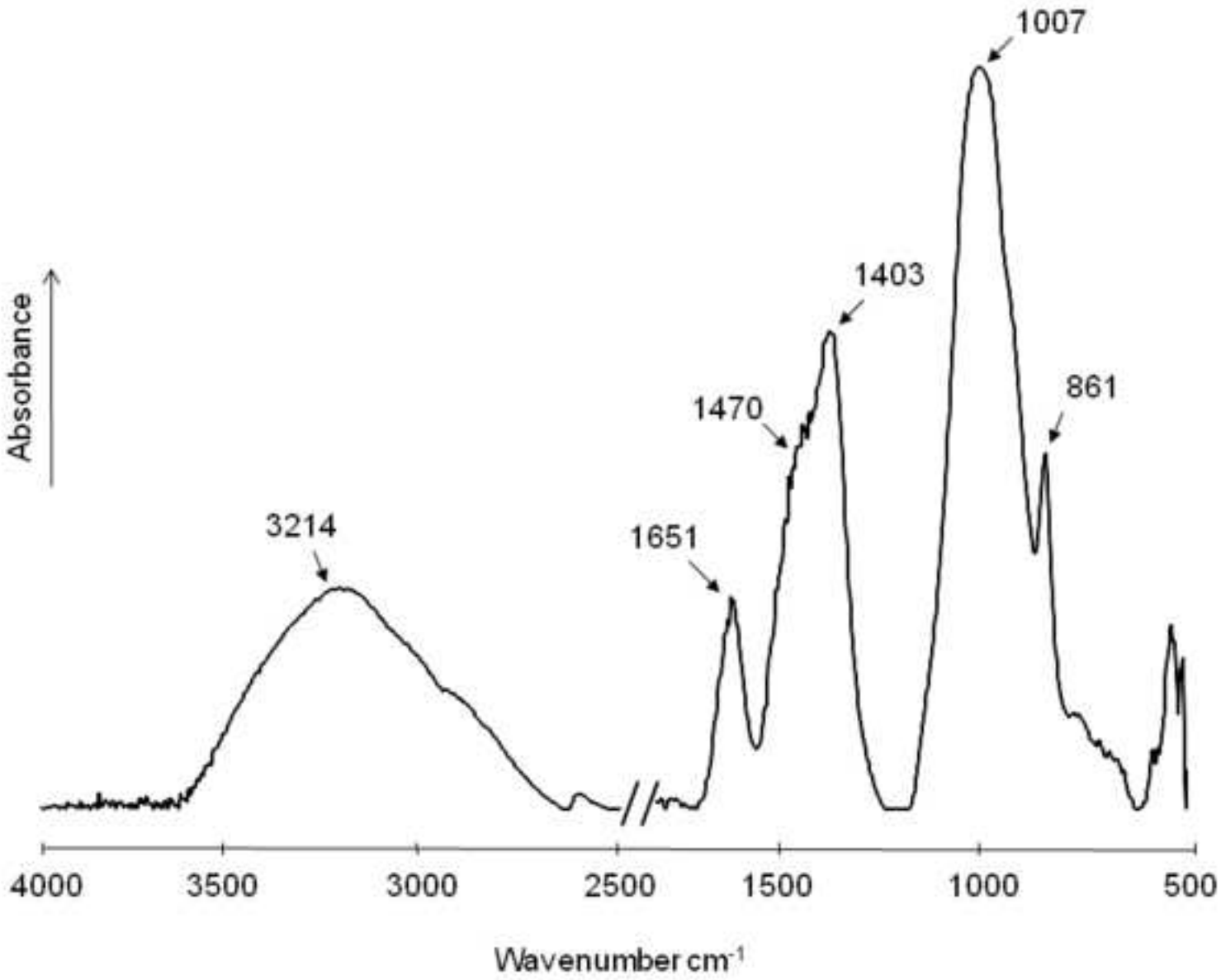
1007
1403
1470
861
3214
1651
Absorbance
4000
3500
3000
2500
1500
1000
500
Wavenumber cm-1